



# 1    **High biodegradability of water-soluble organic carbon in** 2    **soils at the southern margin of the boreal forest**

3    Yuqi Zhu<sup>1,2</sup>, Chao Liu<sup>3</sup>, Rui Liu<sup>1,2</sup>, Hanxi Wang<sup>1,2</sup>, Xiangwen Wu<sup>1,2</sup>, Zihao Zhang<sup>1,2</sup>,  
4    Shuying Zang<sup>1,2\*</sup>, Xiaodong Wu<sup>1,2,4\*</sup>

5    <sup>1</sup>Heilongjiang Provincial Key Laboratory of Geographical Environment Monitoring and Spatial  
6    Information Service in Cold Regions, Harbin Normal University, Harbin, 150025, China

7    <sup>2</sup>Heilongjiang Province Collaborative Innovation Center of Cold Region Ecological Safety, Harbin  
8    150025, China

9    <sup>3</sup>School of Resources and Environment, Northeast Agricultural University, Harbin 150030, China

10    <sup>4</sup>Cryosphere Research Station on Qinghai-Tibet Plateau, Key Laboratory of Cryospheric Science and  
11    Frozen Soil Engineering, Northwest Institute of Eco-Environment and Resources, Chinese Academy of  
12    Sciences, Lanzhou 730020, China

13    *Correspondence to:* Xiaodong Wu (wuxd@lzb.ac.cn), Shuying Zang (zsy6311@hrbnu.edu.cn)

14    **Abstract.** Water-soluble organic carbon (WSOC) is an important component of the organic carbon pool  
15    in boreal ecosystems. However, the biodegradability of WSOC across various soil depths in boreal  
16    ecosystems remains unclear. Here, based on spectroscopic techniques, we conducted a 28-day laboratory  
17    incubation to analyze the molecular composition, biodegradability, and compositional changes of WSOC  
18    at different soil depths in a southern region of the boreal forest. The results showed that in the upper 2 m  
19    soils, the average content of biodegradable WSOC was 0.228 g/kg with an average proportion of 86.41%  
20    in the total WSOC. In the deep soils below 2 m, the average content of biodegradable WSOC content  
21    was 0.144 g/kg, comprising 80.79% of the total WSOC. Spectroscopic analysis indicates that the WSOC  
22    in the upper soils is primarily composed of highly aromatic humic acid-like matter with larger molecular  
23    weights than those in deep soils. Both the aromaticity and molecular weight decrease with depth, and the  
24    WSOC is mainly composed of fulvic acid-like matter in the deep soils, suggesting high biodegradability  
25    of WSOC in the deep soils. Overall, our results suggest that the water-soluble organic carbon in the  
26    boreal forests exhibits high biodegradability both in the shallow layer and deep soils.

## 27    **1 Introduction**

28    Boreal forests cover only around 11% of Earth's land surface, while they store one-third of the global  
29    terrestrial carbon stock (Adamczyk, 2021), and substantial amounts are also present in deep layers  
30    (Bockheim and Hinkel, 2007; Strauss et al., 2017; Schirrmeister et al., 2011). Climate change can



31 influence carbon release and sequestration in these soils (Ohlson et al., 2009; Liang et al., 2024), for  
32 example, through the melting of ground ice, the occurrence of wildfires, and rising soil temperatures  
33 (Zhong et al., 2023; Gao et al., 2021; Zhang et al., 2023; Bond-Lamberty et al., 2007; Kasischke et al.,  
34 1995). These changes also alter the composition of soil microbial communities, affecting their stability  
35 and functional capacity, and ultimately leading to the loss of organic carbon in northern ecosystems  
36 (Zhong et al., 2023; Wu et al., 2021).

37 Water-soluble organic carbon (WSOC) is a complex mixture composed of both high- and low-  
38 molecular-weight compounds, derived from vegetation, litter, root exudates, and microbial biomass and  
39 enzymes (Thurman, 2012; Guggenberger and Zech, 1994). It serves as an important substrate for  
40 microbial activity (Neff and Asner, 2001; Moore, 2003). The bioavailability of WSOC largely depends  
41 on its chemical composition: simple organic compounds such as amino acids, carbohydrates, and fatty  
42 acids are more easily decomposed, whereas more complex components like humic substances require  
43 longer decomposition times (Ma et al., 2019). Most leachates from litter and vegetation are dominated  
44 by low-molecular-weight molecules, which are highly biodegradable and support microbial growth  
45 (Michalzik et al., 2003). Although WSOC accounts for only about 1% of soil organic carbon (SOC)  
46 (Margesin, 2008), it represents the most mobile and bioavailable fraction of SOC (Kaiser and Kalbitz,  
47 2012). Climate change can enhance the release of soil carbon as dissolved organic carbon (DOC) into  
48 surface water (Bowden et al., 2008; Olefeldt and Roulet, 2012). Understanding the dynamics of this  
49 carbon fraction is critical for elucidating SOC turnover in boreal forests (Olefeldt et al., 2014; Öquist et  
50 al., 2014).

51 Due to the cold temperatures, the decomposition rate of soil organic matter (SOM) in boreal forests  
52 is low due to the low soil microbial activity (Walz et al., 2017). Over millennial timescales, frozen  
53 conditions and cryopedogenic processes, such as cryoturbation, have buried organic-rich surface soils  
54 into deep layers, further reducing decomposition rates and promoting long-term carbon sequestration  
55 (Ping et al., 2015). These low decomposition rates result in a high proportion of labile and biodegradable  
56 fractions within soil organic carbon in boreal forests (Song et al., 2020), including water-soluble organic  
57 carbon (Cory et al., 2013). Studies indicate that WSOC in shallow boreal forest soils is highly  
58 biodegradable (Panneer Selvam et al., 2016), with its bioavailability ranging from 24% to 71% (Ma et  
59 al., 2019). However, most of the previous studies focused on WSOC in runoff or soil water rather than



60 in situ conditions, leaving significant knowledge gaps that hinder our ability to predict SOC loss under a  
 61 warming climate.

62 Boreal forest deep soils effectively preserve plant material. This is evidenced by several key  
 63 indicators: as depth increases, the contribution of lignin-derived carbon to total carbon rises, the ratios of  
 64 acid (AC) to aldehyde (AL) of the syringyl (S) and vanillyl (V) units decrease, and there is a continual  
 65 increase in the S/V ratio and plant-derived sugars (Pengerud et al., 2017). As a result, deep soils store a  
 66 significant proportion of labile carbon that can be rapidly mineralized (Drake et al., 2015). In contrast,  
 67 DOC in groundwater from boreal forest predominantly consists of aged, hydrophobic, and recalcitrant  
 68 components, largely driven from stable soil organic matter (Hope et al., 1994). To elucidate the  
 69 mechanisms underlying the varying biodegradability of WSOC in boreal forest regions, it is critical to  
 70 address current knowledge gap regarding the content, chemical composition and biodegradability of in  
 71 situ WSOC in these environments. The object of this study is to quantify the biodegradability of WSOC  
 72 at different soil depths in a boreal forest. We conducted laboratory incubation experiments to determine  
 73 differences in biodegradable water-soluble organic carbon (BWSOC) and employed spectroscopic  
 74 techniques to reveal its compositional characteristics (Kothawala et al., 2014; Chavez-Vergara et al.,  
 75 2014; Sun et al., 2022; Murphy et al., 2008; He et al., 2023). We hypothesized that 1) WSOC from  
 76 shallower soil layers exhibits higher biodegradability and mineralization rates, and 2) the primary factors  
 77 controlling decomposition rates across soil depths are related to the molecular composition of WSOC.

## 78 **2 Materials and methods**

### 79 **2.1 Study area and sample collection**

80 The southern region of the boreal forest is highly sensitive to climate warming (Randerson et al., 2006;  
 81 Zou and Yoshino, 2017; Peng et al., 2022). The forests of the Daxing'an Mountains in Northeast China  
 82 represent the southernmost extent of the boreal forest biome (Jiang et al., 2002; Huang et al., 2010). The  
 83 sampling site (50°24'10.8"N, 120°50'12.9"E) is located within the island permafrost zone (Bockheim,  
 84 2006; Ran et al., 2012; Brown et al., 1997) (Fig. 1). In 2023, the mean average temperature was -1.24°C,  
 85 and the annual precipitation of 290.3 mm (Qweather, [https://www.qweather.com/en/historical/ergun-](https://www.qweather.com/en/historical/ergun-101081014.html)  
 86 [101081014.html](https://www.qweather.com/en/historical/ergun-101081014.html)). The dominant tree species in the study area is *Betula platyphylla*, which characterizes  
 87 the typical local forest ecosystem (Zou and Yoshino, 2017; Jiang et al., 2002).

88 During July 9th-11th, 2023, a soil column (13.5 cm in diameter) was collected from a piedmont terrace



89 at an elevation of 734 m. The column extended to a depth of 740 cm and was divided into 12 layers (L1–  
 90 L12). Soil texture was determined in the field using the “texture-by-feel” estimation method (Vos et al.,  
 91 2016). Soil color was recorded using the Munsell Soil Color Chart (Table 1). There is structural ice in at  
 92 the depth between 160-180 cm. Although we could not verify whether this area has permafrost because  
 93 we lack the ground monitoring data, this site represents the southern margin of the boreal forests.

94 **Table 1. Depths, soil colors (Munsell color system), textures (based on “texture-by-feel”**

95 **estimation ) of soil samples**

Named	Depth	Soil color	Soil texture
L1	0-10 cm	10YR 2/1	Heavy loam
L2	10-20 cm	10YR 2/1	Heavy loam
L3	20-30 cm	10YR 2/1	Heavy loam
L4	30-60 cm	7.5YR 2.5/1	Silty clay Loam
L5	60-90 cm	7.5YR 2.5/1	Silty clay Loam
L6	90-120 cm	7.5YR 2.5/1	Silty clay Loam
L7	120-150 cm	7.5YR 2.5/1	Silty clay Loam
L8	150-160 cm	7.5YR 2.5/1	Silty clay Loam
L9	160-180 cm	7.5YR 2.5/1	Silty clay Loam
L10	220-250 cm	7.5YR 5/2	Silty clay Loam
L11	420-450 cm	10YR 4/3	Sandy clay
L12	700-740 cm	10YR 4/3	Sandy clay

96

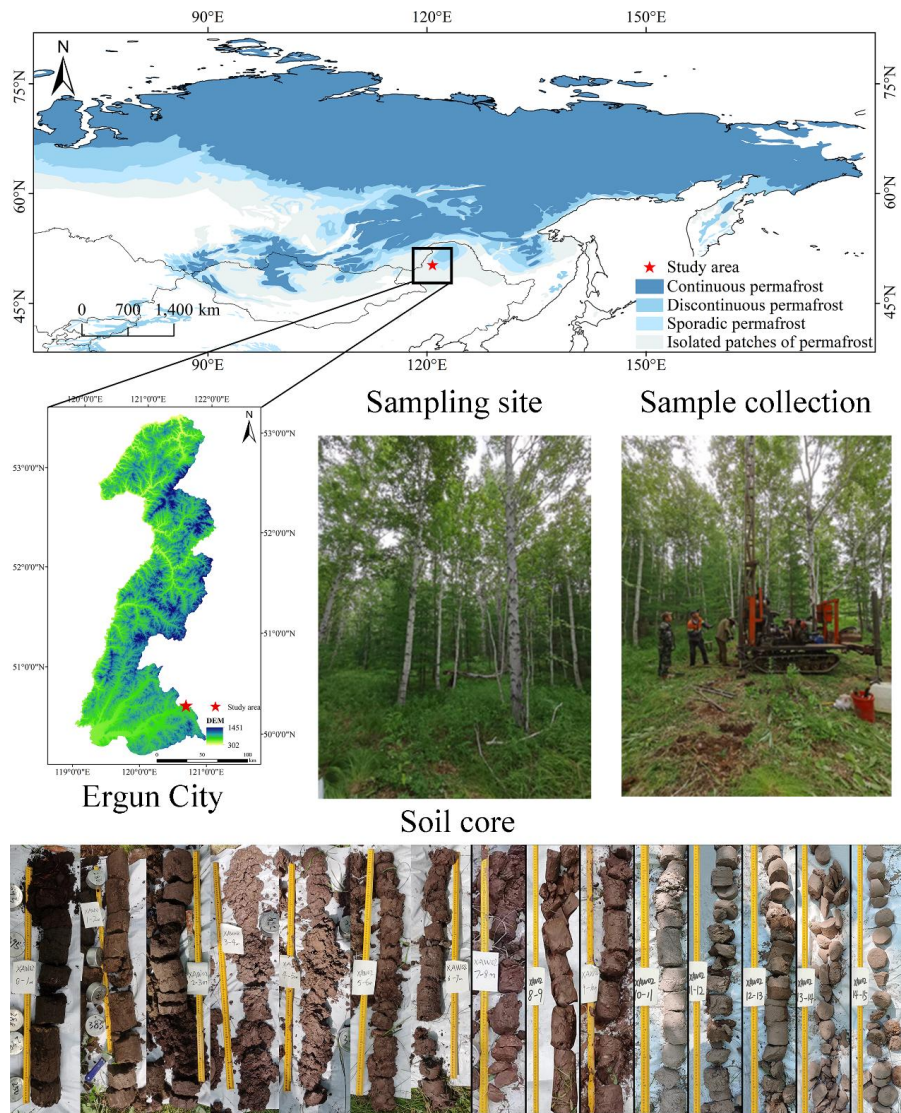


Figure 1. Study area and soil core sample collection. Permafrost distribution is adapted from Circum-Arctic map of permafrost and ground ice condition (Brown et al., 1997).

## 2.2 Physicochemical analysis and spectral analysis of WSOC

Gravimetric soil moisture (GSM) was quantified using the gravimetric method. Soil pH was measured with a PHS-3E pH meter (Leici, China) after shaking a soil-water suspension at a ratio of 1:2.5 (w/v). Soil electrical conductivity (EC) was determined using a DDSJ-319L conductivity meter (Leici, China) with a soil-to-water ratio of 1:5 (w/v). Soil organic carbon (SOC) and total carbon (TC) contents were determined by the dry combustion method using a Multi N/C 3100 analyzer (Jena, Germany) (Nelson



106 and Sommers, 1996). Soil inorganic carbon (SIC) was calculated through differential subtraction.

107 Water-soluble organic carbon (WSOC) was extracted by adding fresh soil samples sieved through a 2  
 108 mm sieve, to deionized water at a ratio of 1:5 (w/v). The mixture was shaken continuously for 4 hours at  
 109 200 r/min and 25°C. The samples were then centrifuged for 15 minutes at 4500 r/min and filtered through  
 110 0.45 µm glass fiber filters (Jones and Willett, 2006). A portion of the filtrate was used for ultraviolet  
 111 spectroscopic analysis, and the remaining filtrate was acidified by adding 3 mol/L hydrochloric acid to  
 112 adjust the pH to  $\leq 2$ , effectively removing inorganic carbon. The pretreated samples were stored at 4°C  
 113 and analyzed within a week using the dry combustion method with a Multi N/C 3100 analyzer (Jena,  
 114 Germany).

115 Total nitrogen (TN) was converted into ammonium nitrogen through an oxidation-reduction reaction  
 116 under the influence of concentrated sulfuric acid, sodium thiosulfate, and a catalyst (Kirk, 1950), and  
 117 quantified using the ammonia nitrogen module of a SAN++ flow injection auto-analyzer (Skalar,  
 118 Holland). Ammonium nitrogen ( $\text{NH}_4^+\text{-N}$ ) and nitrate nitrogen ( $\text{NO}_3^-\text{-N}$ ) were determined after extracting  
 119 2 g of fresh soil into 10 mL of 2 mol/L potassium chloride solution, shaking for 2 hours at 200 r/min,  
 120 then centrifuging for 3 minutes at 8000 r/min and filtering through 0.45 µm glass fiber filters (Li et al.,  
 121 2012).

122 Total phosphorus (TP) in soil was determined using sodium hydroxide to convert all phosphorus-  
 123 containing minerals and organic phosphorus compounds into soluble orthophosphates (Sparks et al.,  
 124 2020), which were then quantified using a SAN++ flow injection auto-analyzer (Skalar, Holland).

125 Different WSOC compounds exhibit distinct spectral properties, and ultraviolet-visible (UV-Vis)  
 126 absorption spectra are commonly used to assess WSOC quality. The absorbance at 254 nm ( $\text{SUAV}_{254}$ ) is  
 127 strongly correlated with WSOC aromaticity (Weishaar et al., 2003). The  $E_{250}/E_{365}$  ratio, indicative of  
 128 WSOC aromaticity, humification degree, and molecular size (Helms et al., 2008), is also an important  
 129 parameter for characterizing WSOC. The absorbance values of WSOC at 250, 254, and 365 nm were  
 130 measured using a Lambda 35 UV/VIS spectrometer (PerkinElmer, USA) with a 10 mm quartz cuvette.  
 131 For each sample, the  $\text{SUAV}_{254}$  value was calculated by dividing the UV absorbance measured at 254 nm  
 132 by the WSOC concentration and multiplying 100 (Weishaar et al., 2003). The  $E_{250}/E_{365}$  ratio was  
 133 obtained by dividing the absorbance value at 250 nm by that at 365 nm (Helms et al., 2008). Throughout  
 134 the incubation period, including the initial measurement on Day 0, UV-Vis spectroscopy was conducted



on a portion of the WSOC extract to assess quality parameters such as  $SUVA_{254}$  and the  $E_{250}/E_{365}$  ratio. Moreover, compared to UV spectra, the excitation-emission matrix (EEM) generated from continuous fluorescence scans provides multidimensional information with higher sensitivity for detecting low concentrations of organic matter (Anumol et al., 2015; Sgroi et al., 2018). This study employs three-dimensional fluorescence spectroscopy to further explore the composition of water-extracted organic matter (WEOM), dividing the fluorescence spectra into five regions based on integrated fluorescence area (Chen et al., 2003) (Table S1.). WEOM was extracted by adding deionized water to fresh soil samples sieved through a 2 mm sieve at a soil-to-water ratio of 1:5 (w/v), followed by shaking at 200 r/min for 24 hours at 25°C. The samples were then centrifuged at 4500 r/min for 15 minutes, and the supernatant was filtered through a 0.45  $\mu$ m glass fiber filter to obtain WEOM (Zhou et al., 2023). A three-dimensional fluorescence spectrophotometer (Aqualog, HORIBA Scientific, France) was used to identify the fluorescent substances in water soluble organic matter. The excitation wavelength was set from 200 to 450 nm and the emission wavelength from 250 to 550 nm, with both the excitation and emission sampling intervals and slits adjusted to 5 nm, and the scanning speed maintained at 12,000 nm/min.

### 2.3 Laboratory Incubation experiment

In the laboratory incubation experiments, we assessed the biodegradable water-soluble organic carbon (BWSOC) at various soil depths over a period of 28 days, with measurements of WSOC content taken on days 0, 2, 7, 14, and 28 (Vonk et al., 2015; Mu et al., 2017).

To minimize variability, WSOC samples were extracted in bulk from each soil layer. Fresh soil samples, sieved through a 2 mm sieve, were mixed with deionized water at a soil-to-water ratio of 1:5 (w/v), shaken continuously at 200 r/min and 25°C for 4 hours, centrifuged at 4500 r/min for 15 minutes, and filtered through 0.45  $\mu$ m filters. The resulting WSOC solution (500 mL) from each soil layer was thoroughly homogenized. Aliquots of 30 mL of the homogenized WSOC solution were transferred into 50 mL sterile serum bottles.

To prepare the microbial inoculum, fresh soil samples from each soil layer were sieved through a 2 mm sieve to remove debris and large particles. The sieved soil was mixed with sterile deionized water at a ratio of 1:5 (w/v) and shaken continuously at 200 r/min and 25°C for 4 hours. This process facilitated the release of microorganisms from soil particles into the aqueous phase, allowing them to enter the extract in suspension form (Bottomley et al., 2020). The suspension was then centrifuged at 4500 r/min





164 for 15 minutes to remove any remaining soil particles. The supernatant was filtered through pre-  
 165 combusted (450°C for over 4 hours) Whatman GF/C filters with a pore size of 1.2 µm to obtain the  
 166 microbial inoculum. Finally, 3 mL of the inoculum (constituting 10% of the total volume) was added to  
 167 the water samples to introduce indigenous soil microorganisms from the respective soil depths (Vonk et  
 168 al., 2015).

169 To minimize nutrient limitations on microbial activity, standardized amounts of ammonium nitrate  
 170 ( $\text{NH}_4\text{NO}_3$ ) and dipotassium hydrogen phosphate ( $\text{K}_2\text{HPO}_4$ ) were added to each sample. Specifically, a  
 171 0.02674 mol/L  $\text{NH}_4\text{NO}_3$  stock solution was prepared by dissolving 2.14 g of  $\text{NH}_4\text{NO}_3$  in 1 L of deionized  
 172 water. Then, 100 µL of this stock solution was added to each 33 mL sample, resulting in final  
 173 concentrations of approximately 80 µmol/L for  $\text{NH}_4^+$  and  $\text{NO}_3^-$ . Similarly, a 0.0334 mol/L  $\text{K}_2\text{HPO}_4$  stock  
 174 solution was prepared by dissolving 5.8176 g of  $\text{K}_2\text{HPO}_4$  in 1 L of deionized water, which was  
 175 subsequently diluted tenfold to obtain a 0.00334 mol/L working solution. We added 100 µL of the diluted  
 176  $\text{K}_2\text{HPO}_4$  solution to each sample, achieving a final  $\text{PO}_4^{3-}$  concentration of approximately 10 µmol/L.  
 177 These nutrient concentrations were chosen based on previous studies (Mu et al., 2017; Vonk et al., 2015),  
 178 which demonstrated that they are sufficient to prevent nutrient limitation without causing nutrient  
 179 saturation. By adding equal amounts of nutrients to all samples, we standardized nutrient availability  
 180 across different soil layers, minimizing potential variability due to inherent nutrient contents. This  
 181 approach allows us to focus on the effects of WSOC characteristics on microbial activity. Each sample  
 182 was incubated in triplicate, along with two control blanks: one with deionized water and another with  
 183 deionized water plus nutrients, for a total of five samples per depth interval. All samples were incubated  
 184 at 20°C in the dark in a constant temperature incubator (Thermo, USA), with caps partially opened. The  
 185 samples were shaken once daily to maintain aerobic conditions.

186 On measurement days, the samples were re-filtered through a 0.45 µm glass fiber filter to exclude  
 187 filterable microbial biomass. The quantified WSOC degradation accounted for both microbial  
 188 mineralization and assimilation processes. Part of the samples was immediately used for absorbance  
 189 measurements at wavelengths of 250 nm, 254 nm, and 365 nm. Another portion was acidified using 3  
 190 mol/L hydrochloric acid to adjust the pH to  $\leq 2$  and subsequently stored at 4°C, with WSOC concentration  
 191 measured within a week. BWSOC was determined by subtracting the WSOC content on day 28 from the  
 192 WSOC content on day 0. BWSOC (%) was calculated by dividing BWSOC by the WSOC content on





193 day 0 and multiplying by 100 %. The formulas for calculating BWSOC and BWSOC (%) are provided  
194 in the Supporting Information. All experimental procedures were conducted on a sterile laminar flow  
195 bench.

#### 196 **2.4 Data analysis**

197 Pearson correlation analysis was used to explore the relationships between various environmental  
198 factors and characteristics of WSOC. One-way ANOVA was employed to test the significant differences  
199 in the molecular composition of WSOC, which was indicated by the  $SUVA_{254}$  and  $E250/E365$  ratios,  
200 across different soil depth. To compare the differences in biodegradable water-soluble organic carbon  
201 (BWSOC) across soil depths, the non-parametric Kruskal-Wallis test was applied. The biodegradability  
202 of water-soluble organic carbon at time (BWSOC<sub>t</sub>) was underwent nonlinear exponential fitting to obtain  
203 the reaction kinetics constant ( $k$ ). All statistical analyses were performed using R version 4.4.0  
204 (<https://www.r-project.org/>).

### 205 **3 Results**

#### 206 **3.1 Physicochemical properties**

207 The concentration of nutrients in the soil gradually decreases with depth (Fig. 2). In the surface  
208 layer (0-30 cm), nitrogen content is lowest at the 10-20 cm depth. Electrical conductivity and total  
209 phosphorus content are highest at 700-740 cm. The WSOC content ranged from 0.123 g/kg to 0.355 g/kg.  
210 On average, WSOC content was 0.246 g/kg in the upper 0–2 m layer, while below 2 m it decreased to an  
211 average of 0.183 g/kg. The highest WSOC content, at 0.355 g/kg, was observed between 160–180 cm.

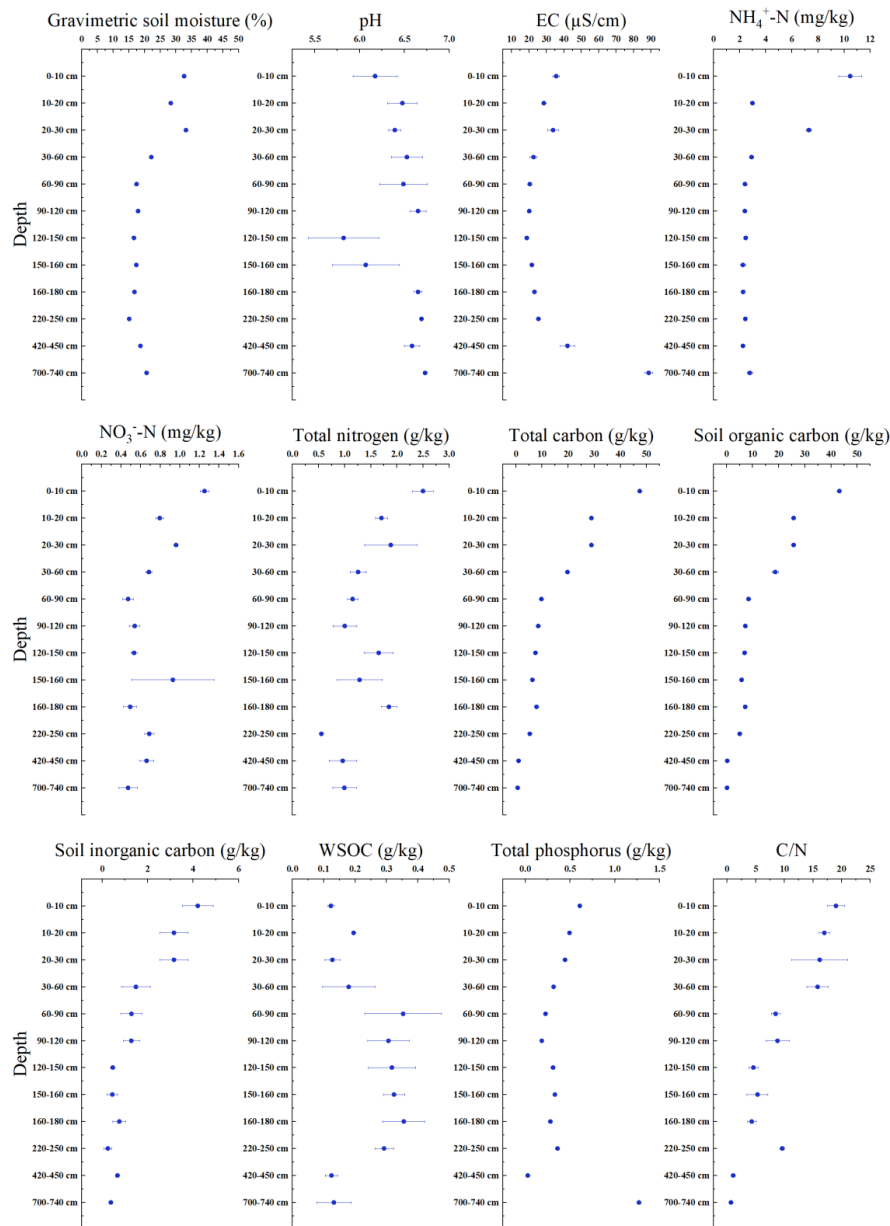


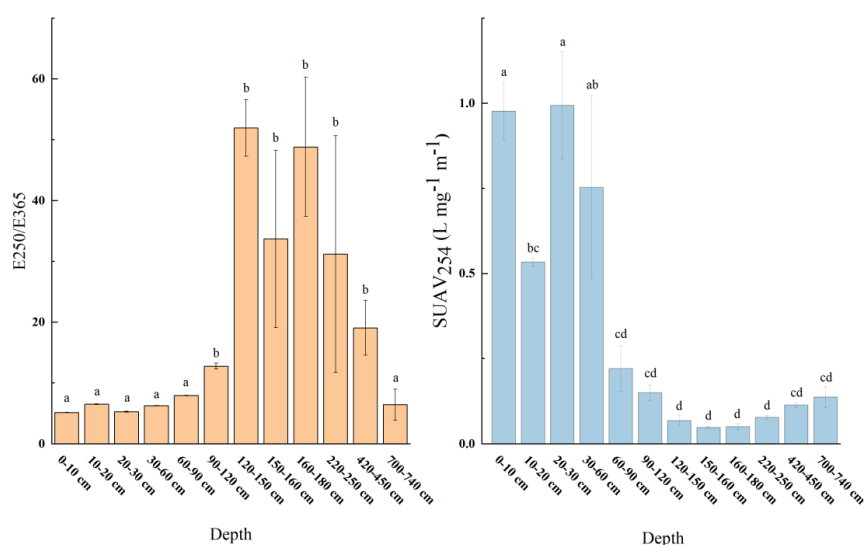
Figure 2. Soil physicochemical characteristics at different depth, error bars represent the standard error (n=3).

### 3.2 Spectroscopy of water-soluble organic carbon

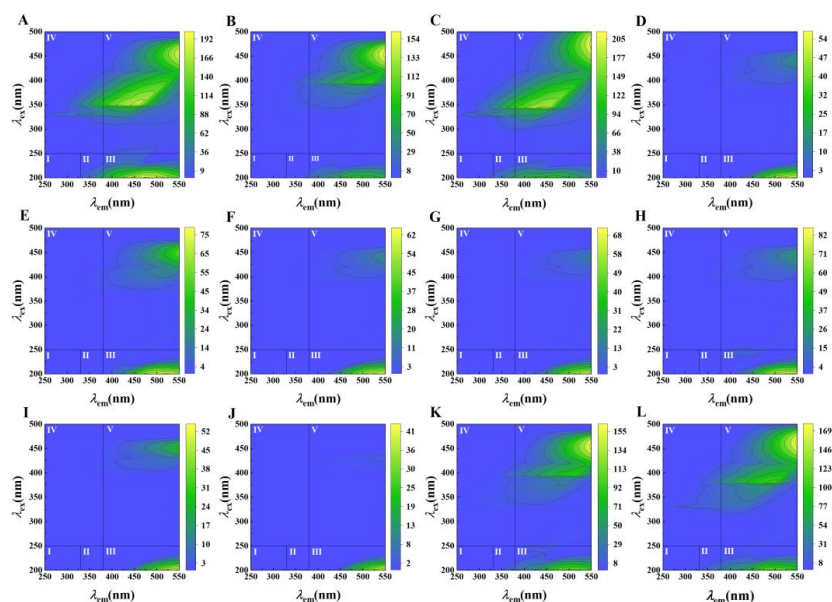
There were significant differences in the aromaticity and molecular weight of WSOC between the



217 0-60 cm depth and deeper layers within the boreal forest ecosystem ( $n=3$ ,  $p<0.05$ ) (Fig. 3). The WSOC  
 218 in the 0-60 cm depth predominantly consists of components with higher aromaticity and larger molecular  
 219 weights. In contrast, deeper layers have WSOC with smaller molecular weights and less aromaticity (Fig.  
 220 3). Additionally, three-dimensional fluorescence spectroscopy displayed two major fluorescence peaks  
 221 (Fig. 4): one in Region III, representing fulvic acid-like matter, and another in Region V, representing  
 222 humic acid-like matter. The fluorescence intensity of fulvic acids is high across all depths, with  
 223 significantly greater intensity in the 0-30 cm and 420-740 cm depths compared to other depths (Fig. 5).



224  
 225 Figure 3.  $E_{250}/E_{365}$  and  $SUAV_{254}$  at different depths. Different letters represent significant differences  
 226 among different sampling points ( $n=3$ ,  $p < 0.05$ ), error bars represent the standard error.



227  
 228 Figure 4. EEM fluorescence spectra of WSOM at different depths. Regions I, II, III, IV, and V are,  
 229 respectively, for tyrosine-like aromatic protein, tryptophan-like aromatic protein, fulvic acid-like matter,  
 230 soluble microbial byproduct-like matter, and humic acid-like matter. A: (0-10 cm); B: (10-20 cm); C:  
 231 (20-30 cm); D: (30-60 cm); E: (60-90 cm); F: (90-120 cm); G: (120-150 cm); H: (150-160 cm); I: (160-  
 232 180 cm); J: (220-250 cm); K: (420-450 cm); L: (700-740 cm).

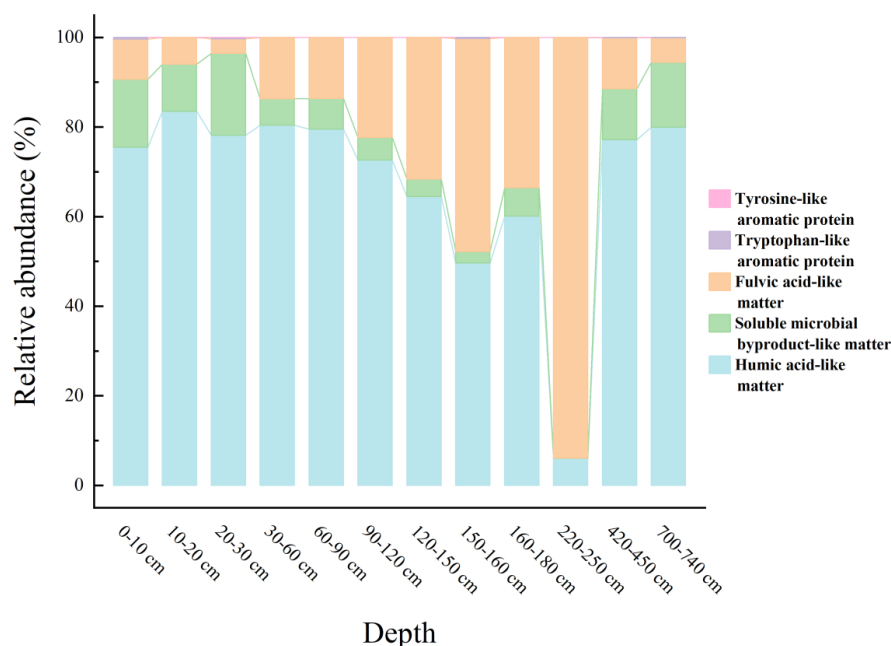


Figure 5. The EEM fluorescence spectra of WSOC at different depths

### 3.3 Biodegradable water-soluble organic carbon, and the reaction kinetics constant $k$

The soils of 60-180 cm depth exhibited higher BWSOC content and degradability compared to other depths (Fig. 6). Significant variations in degradation rates were observed during the incubation process. The reaction kinetics constant ( $k$  values) indicated that WSOC degradation in deeper soils proceeded more slowly (Table 2), occurring predominantly between days 14 and 28 of incubation. In contrast, the WSOC at 60-90 cm depth decomposed rapidly during the early stages of incubation, with a  $k$  value of 1.0952 (1/day). In summary, although deeper soils also contain relatively high BWSOC content, decomposition in these layers occurs primarily during the later stages of incubation (days 14–28), whereas the WSOC in upper layers is rapidly decomposed at the beginning of the incubation period (Fig. 7).

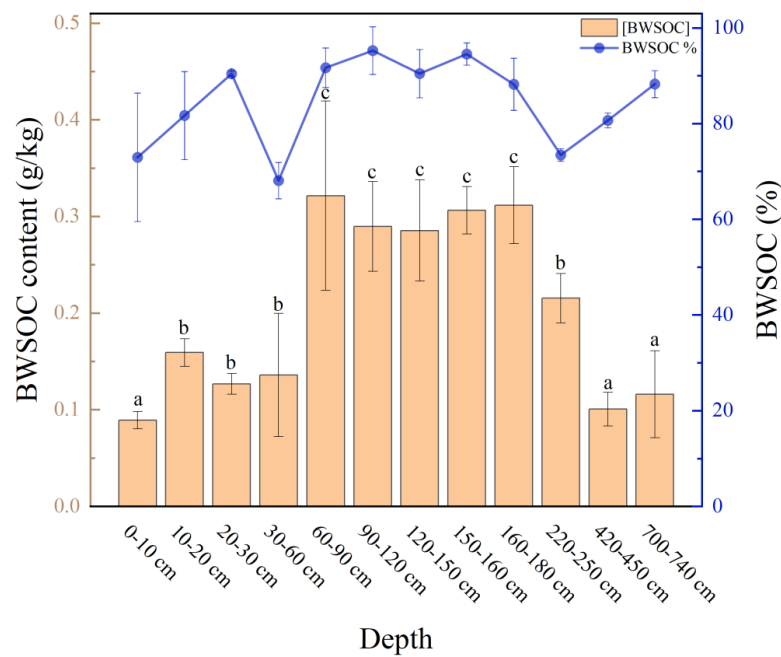
**Table 2. Content of BWSOC, BWSOC (%), reaction kinetics constant ( $k$ ), and coefficient of determination ( $R^2$ ) at different soil depths.**

Depth	BWSOC (g/kg)	BWSOC (%)	$k$ (1/d)	$R^2$
0-10 cm	0.089±0.009	72.96%±13.41%	0.0497	0.9394



10-20 cm	0.159±0.014	81.68%±9.18%	0.4991	0.7484
20-30 cm	0.127±0.011	90.43%±0.55%	0.1302	0.8735
30-60 cm	0.136±0.064	68.08%±3.79%	0.3604	0.5532
60-90 cm	0.321±0.098	91.67%±4.14%	1.0952	0.9847
90-120 cm	0.290±0.046	95.25%±4.98%	0.3651	0.9360
120-150 cm	0.285±0.052	90.45%±5.05%	0.1394	0.8549
150-160 cm	0.306±0.025	94.54%±2.32%	0.0601	0.8823
160-180 cm	0.311±0.040	88.21%±5.45%	0.0737	0.9058
220-250 cm	0.215±0.026	73.46%±1.31%	0.0863	0.8910
420-450 cm	0.101±0.017	80.66%±1.55%	0.0712	0.9747
700-740 cm	0.116±0.045	88.25%±2.81%	0.0681	0.8692

247



248

249 Figure. 6 Content of biodegradable water-soluble organic carbon (BWSOC) and the percentage of  
250 biodegradable water-soluble organic carbon (BWSOC%) at different depths, error bars represent the  
251 standard error (n=3).

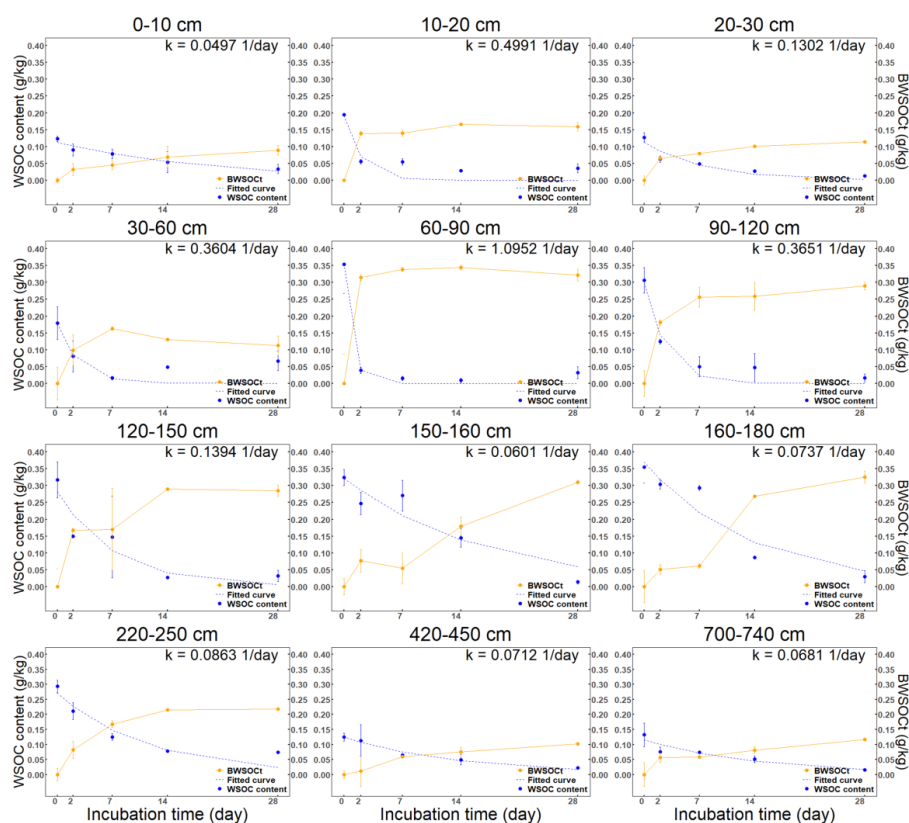


Figure 7. Water-soluble organic carbon content during the 28-day incubation at various depths. The blue curve is a nonlinear exponential fitting of WSOC content. The yellow curve illustrates the changes in biodegradable water-soluble organic carbon (BWSOC), with the  $k$ -value representing the reaction kinetics constant, error bars represent the standard error ( $n=3$ ).

At 160-180 cm depth,  $SUAV_{254}$  values gradually increased over the incubation period, while  $E_{250}/E_{365}$  value steadily decreases (Fig. 8). This indicates that as the incubation time increases, the aromaticity and molecular weight of the remaining WSOC also increase. In contrast, WSOC at other depths is rapidly decomposed during the initial stages of incubation, leading to a quick increase in  $SUAV_{254}$  and a rapid decrease in  $E_{250}/E_{365}$  in the first 0-7 days, reflecting the rapid utilization of smaller, less aromatic molecules early in the incubation. The WSOC content at depths of 60-120 cm and the absorbance values at depths of 220-740 cm were extremely low by day 28, which likely resulted in very





low SUVA<sub>254</sub> and *E250/E365* values on that day. As a result, we excluded these data from the analysis.

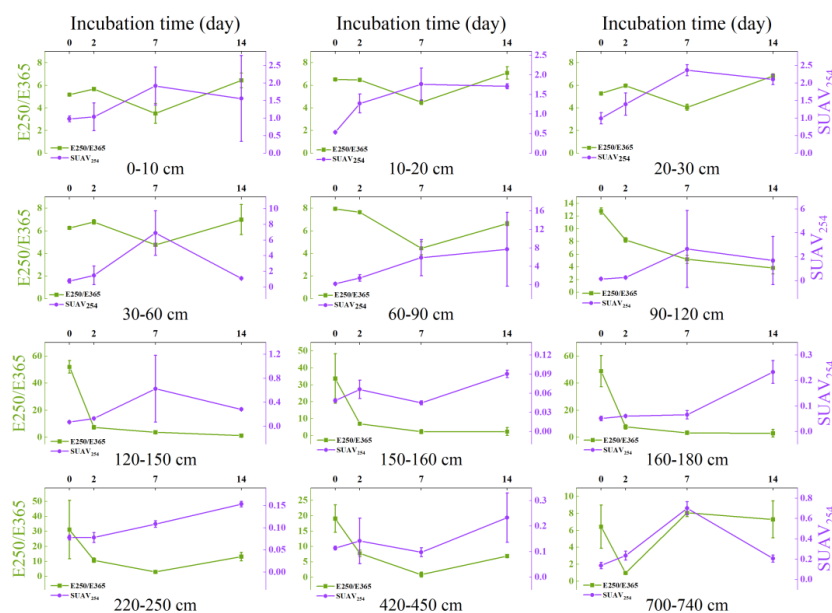


Figure 8. Water soluble organic carbon *E250/E365* and SUVA<sub>254</sub> during the 14 days of incubation at different soil depths, error bars represent the standard error.

### 3.4 Relationship among the biodegradation of water-soluble organic carbon and environmental factors

Total carbon (TC), total nitrogen (TN), WSOC and its degradability showed significantly negative correlations with depth. The aromaticity of WSOC (SUVA<sub>254</sub>) and molecular weight (*E250/E365*) showed significant correlations with biodegradable water-soluble organic carbon (BWSOC). *E250/E365* showed a positive correlation with BWSOC ( $r = 0.528$ ), while SUVA<sub>254</sub> was negatively correlated with BWSOC ( $r = -0.582$ ). Additionally, SUVA<sub>254</sub> and *E250/E365* demonstrated a strong negative correlation ( $r = -0.589$ ), suggesting that the molecular composition of WSOC significantly impacts its biodegradability. The degradation rate ( $k$ ) and the degree of biodegradability (BWSOC %) of WSOC has no significant correlations with other environmental factors (Fig. 9).

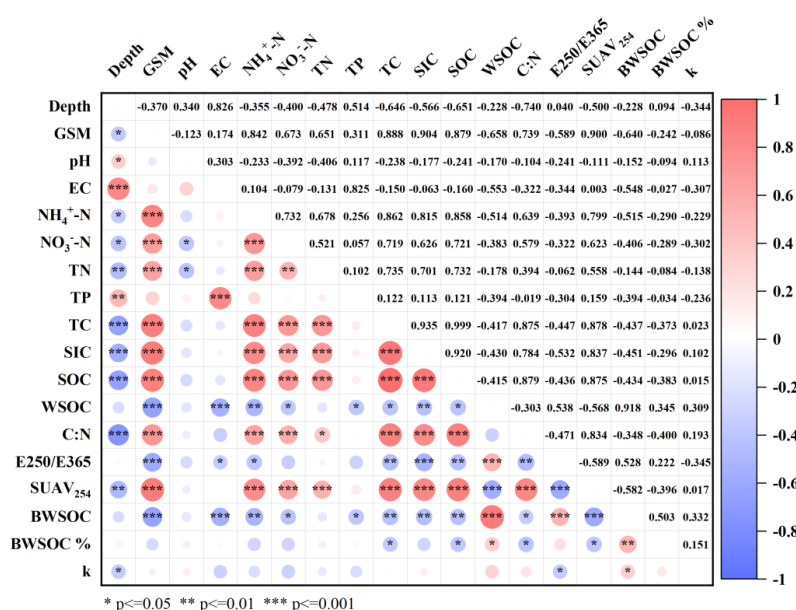


Figure 9. Correlation coefficients among different environmental factors (n=12). Red indicates a positive correlation, while blue indicates a negative correlation. The deeper the color, the stronger the correlation. The color gradient ranges from -1 (complete negative correlation) to +1 (complete positive correlation).

## 4 Discussion

### 4.1 Water-soluble organic carbon content and spectral signature

At depths of 60–180 cm, WSOC concentrations were relatively higher than in other soil layers. This pattern is plausible since higher organic matter inputs from roots and litter generally occur in these upper soil layers, facilitating WSOC accumulation (Hu et al., 2014). Additionally, the silty clay loam texture at these depths contains a substantial proportion of silt and clay particles, creating a denser pore structure capable of effectively adsorbing and retaining organic matter (Bucka et al., 2023). With increasing soil depth, the higher sand content can lead to lower porosity but higher macroporosity (Mentges et al., 2016). Consequently, higher sand content reduces the potential for SOC preservation (Bucka et al., 2023), resulting in lower WSOC concentrations in deeper layers.

We found that the WSOC in the 0–60 cm soil layer exhibited stronger aromaticity and larger molecular weight. Three-dimensional fluorescence spectroscopy confirmed that the WSOC in the surface layer was primarily composed of larger molecular humic substances, which aligns with previous findings from



295 boreal forests in Alaska (Wickland et al., 2007). These substances are primarily plant-derived (Walker et  
 296 al., 2013; Mann et al., 2016) and are often associated with root exudates and microbial exometabolites  
 297 abundant in the upper soil horizons (Raudina et al., 2017).

298 Deep soils exhibited a higher proportion of fulvic-like substances in their WSOC, characterized by  
 299 smaller molecular weights and lower aromaticity. This finding suggests that WSOC in deeper layers  
 300 generally possesses lower aromaticity and molecular weight (Fouche et al., 2020). Although SOC in deep  
 301 soils is usually considered has high fresh organic materials due to the low temperature limits the microbial  
 302 decomposition (Heffernan et al., 2024), our results suggest that long term accumulation of highly  
 303 decomposed organic matter that forms low-molecular-weight fulvic acid-like substances with lower  
 304 aromaticity is still abundant in deep soils (Corvasce et al., 2006; Lv et al., 2020). This mechanism helps  
 305 explain the observed decrease in WSOC aromaticity and molecular weight with increasing soil depth  
 306 (Koven et al., 2015; Panneer Selvam et al., 2017; Drake et al., 2015).

#### 307 **4.2 Biodegradable water-soluble organic carbon, and the reaction kinetics constant $k$**

308 Water-soluble organic carbon (WSOC) in the boreal forests demonstrates high biodegradability,  
 309 with the highest biodegradability of WSOC in the 60-160 cm. In Alaska's Kolyma River basin, WSOC  
 310 concentrations decreased by about 50% following a seven-day incubation (Spencer et al., 2015).  
 311 Similarly, in deep Alaskan soils, ancient low-molecular-weight organic acids within WSOC are rapidly  
 312 mineralized, leading to a ~53% decline in WSOC after 200 hours of incubation (Koven et al., 2015). The  
 313 high biodegradability of WSOC is closely related to its chemical composition (Burd et al., 2020). In these  
 314 regions, WSOC primarily consists of low-aromaticity, low-molecular-weight organic matter that is  
 315 readily decomposed by microbes (Drake et al., 2015). making it easily accessible for microbial utilization  
 316 (Ward and Cory, 2015).

317 Despite the high biodegradability of WSOC, decomposition rates in the deeper soils remained  
 318 slower than those in the upper layers, particularly during the later stages of incubation. This pattern  
 319 suggests that microbes rapidly consumed the most bioavailable compounds in the deeper layers at the  
 320 start of the incubation period (Wild et al., 2014). Over time, the residual WSOC became increasingly  
 321 aromatic, indicating that microbes had preferentially utilized the more easily decomposable organic  
 322 matter early on (Drake et al., 2015).

323 Across the soil depth increase, the aromaticity and molecular weight of WSOC decrease,



324 contributing to faster degradation rates (Kalbitz et al., 2003a), particularly during the first 48 hours  
 325 (Roehm et al., 2009).

326 Our study highlights the differences in the biodegradability of WSOC at various soil depths in boreal  
 327 forest ecosystems. However, it is important to note that the high measurements of biodegradable WSOC  
 328 (BWSOC) and BWSOC (%) observed in this study may be influenced by several methodological factors  
 329 (Dutta et al., 2006; Vonk et al., 2015; Abbott et al., 2014; Kaplan and Newbold, 1995; Frias et al., 1995).  
 330 In our study, nutrient amendments were added, and the samples were incubated under aerobic conditions  
 331 at a constant temperature of 20°C in the dark. As a result, the higher BWSOC (%) values observed in  
 332 this study showed the potential decomposition of WSOC rather than the actual decomposition rates under  
 333 natural conditions (Vonk et al., 2015).

#### 334 **4.3 Water-soluble organic carbon biodegradation and environmental factors**

335 BWSOC in this study showed a negative correlation with environmental factors. WSOC and  
 336 BWSOC were significantly positively correlated, collectively confirming that both the molecular  
 337 composition and concentration of WSOC jointly control the biodegradability of water-soluble organic  
 338 carbon (Wang et al., 2024). In addition, electrical conductivity showed a negative correlation with  
 339 BWSOC, which has also been reported in previous studies (Qu et al., 2018). This pattern can be explained  
 340 by the fact that an increase in salinity inhibits microbial degradation of water-soluble organic carbon  
 341 (Yang et al., 2018). Furthermore, BWSOC was negatively correlated with ammonium nitrogen, nitrate  
 342 nitrogen, and total phosphorus, which are key nutrients. One possible explanation is that higher nutrients  
 343 favor the growth of microbes (Ye et al., 2015; Jiang et al., 2024).

344 A significant correlation was also observed between BWSOC and both  $SUAV_{254}$  and the  $E250/E365$   
 345 ratio. These results highlight the importance of WSOC properties in determining its biodegradability  
 346 (Kalbitz et al., 2003b; Fellman et al., 2008). The composition of WSOC is influenced by environmental  
 347 factors such as total carbon, total nitrogen, total phosphorus, and pH (Li et al., 2018; Roth et al., 2019).  
 348 The strong positive correlation between these environmental factors and  $SUAV_{254}$  and  $E250/E365$  can  
 349 be attributed to the high concentration of nutrients, which promotes the accumulation and transformation  
 350 of organic matter, leading to the formation of more complex and recalcitrant organic compounds (Takaki  
 351 et al., 2022).

#### 352 **5 Conclusion**



353 This study quantitatively analyzed the biodegradability of water-soluble organic carbon (WSOC) at  
 354 various depths in a boreal forest. Our results show that BWSOC content ranges from 0.089 g/kg to 0.321  
 355 g/kg, with the lowest observed biodegradability in surface soil WSOC still reaching 68.08%.  
 356 Spectroscopic analyses revealed that surface-layer WSOC predominantly consists of highly aromatic,  
 357 humic acid-like substances. As soil depth increases, the aromaticity and molecular weight of WSOC  
 358 decrease continuously. Concurrently, the proportion of low-molecular-weight, fulvic acid-like substances  
 359 rises, leading to biodegradability values in deeper soils (below 2 m) reaching up to 80.79%. Although  
 360 the WSOC degradation rate in deep soils is significantly lower than that in the upper layers, the WSOC  
 361 at depth remains highly biodegradable. Correlation analyses further indicate that the molecular  
 362 composition of WSOC is a key factor influencing its biodegradability. Overall, our findings suggest that  
 363 WSOC content at the southern boundary of the boreal forest is comparable to that found at higher  
 364 latitudes. Given that WSOC represents the most dynamic fraction of the soil organic carbon pool,  
 365 ongoing climate warming will likely drive substantial SOC losses across multiple soil depths in boreal  
 366 forests.

367

### 368 **Acknowledgements**

369 Thanks to Northwest Institute of Eco-Environment and Resources, Chinese Academy of Sciences for  
 370 sharing the samples and support.

### 371 **Author contributions**

372 **Yuqi Zhu:** Conceptualization, Formal analysis, Investigation, Methodology, Writing – original draft.  
 373 **Xiaodong Wu:** Writing – review and editing, Project administration. **Chao Liu:** Supervision, Validation,  
 374 Resources. **Rui Liu:** Validation, Resources. **Xiangwen Wu:** Resources, Funding acquisition. **Zihao**  
 375 **Zhang:** Validation, Investigation. **Hanxi Wang:** Validation, Resources. **Shuying Zang:** Writing – review  
 376 and editing, Project administration, Data curation, Resources, Funding acquisition.

### 377 **Funding sources**

378 The Science & Technology Fundamental Resources Investigation Program (2022FY100701), National  
 379 Natural Science Foundation of China (U20A2082, 42430412, 32061143032), Basic scientific research  
 380 business expenses of colleges and universities in Heilongjiang Province (2022KYYWF0181), Harbin  
 381 Normal University Postgraduate Innovation Program (HSDSSCX2022108)



## 382 Declaration of Competing Interest

383 The authors declare that they have no known competing financial interests or personal relationships that  
 384 could have appeared to influence the work reported in this paper.

## 385 Data availability

386 Data will be made available on request.

387

388

## 389 Reference

- 390 Abbott, B. W., Larouche, J. R., Jones, J. B., Bowden, W. B., and Balser, A. W.: Elevated dissolved organic  
 391 carbon biodegradability from thawing and collapsing permafrost, *Journal of Geophysical Research:*  
 392 *Biogeosciences*, 119, 2049-2063, 10.1002/2014jg002678, 2014.
- 393 Adamczyk, B.: How do boreal forest soils store carbon?, *BioEssays*, 43, 2100010, 2021.
- 394 Anumol, T., Sgroi, M., Park, M., Roccaro, P., and Snyder, S. A.: Predicting trace organic compound  
 395 breakthrough in granular activated carbon using fluorescence and UV absorbance as surrogates, *Water*  
 396 *Res.*, 76, 76-87, 10.1016/j.watres.2015.02.019, 2015.
- 397 Bockheim, J. G.: Permafrost distribution in the southern circumpolar region and its relation to the  
 398 environment: A review and recommendations for further research, *Permafrost and Periglacial Processes*,  
 399 6, 27-45, 10.1002/ppp.3430060105, 2006.
- 400 Bockheim, J. G. and Hinkel, K. M.: The Importance of “Deep” Organic Carbon in Permafrost-Affected  
 401 Soils of Arctic Alaska, *Soil Science Society of America Journal*, 71, 1889-1892,  
 402 10.2136/sssaj2007.0070N, 2007.
- 403 Bond-Lamberty, B., Peckham, S. D., Ahl, D. E., and Gower, S. T.: Fire as the dominant driver of central  
 404 Canadian boreal forest carbon balance, *Nature*, 450, 89-92, 10.1038/nature06272, 2007.
- 405 Bottomley, P. J., Angle, J. S., and Weaver, R.: *Methods of soil analysis, Part 2: Microbiological and*  
 406 *biochemical properties*, John Wiley & Sons 2020.
- 407 Bowden, W. B., Gooseff, M. N., Balser, A., Green, A., Peterson, B. J., and Bradford, J.: Sediment and  
 408 nutrient delivery from thermokarst features in the foothills of the North Slope, Alaska: Potential impacts  
 409 on headwater stream ecosystems, *Journal of Geophysical Research: Biogeosciences*, 113,  
 410 10.1029/2007jg000470, 2008.
- 411 Brown, J., Sidlauskas, F. J., and Delinski, G.: Circum-arctic map of permafrost and ground ice conditions,  
 412 1997.
- 413 Bucka, F. B., Felde, V. J. M. N. L., Peth, S., and Kögel-Knabner, I.: Complementary effects of sorption  
 414 and biochemical processing of dissolved organic matter for emerging structure formation controlled by  
 415 soil texture, *Journal of Plant Nutrition and Soil Science*, 187, 51-62, 10.1002/jpln.202200391, 2023.
- 416 Burd, K., Estop-Aragónés, C., Tank, S. E., Olefeldt, D., and Naeth, M. A.: Lability of dissolved organic  
 417 carbon from boreal peatlands: interactions between permafrost thaw, wildfire, and season, *Canadian*  
 418 *Journal of Soil Science*, 100, 503-515, 10.1139/cjss-2019-0154, 2020.
- 419 Chavez-Vergara, B., Merino, A., Vázquez-Marrufo, G., and García-Oliva, F.: Organic matter dynamics  
 420 and microbial activity during decomposition of forest floor under two native neotropical oak species in  
 421 a temperate deciduous forest in Mexico, *Geoderma*, 235-236, 133-145, 10.1016/j.geoderma.2014.07.005,



- 2014.
- Chen, W., Westerhoff, P., Leenheer, J. A., and Booksh, K.: Fluorescence Excitation–Emission Matrix Regional Integration to Quantify Spectra for Dissolved Organic Matter, *Environmental Science & Technology*, 37, 5701–5710, 10.1021/es034354c, 2003.
- Corvasce, M., Zsolnay, A., D’Orazio, V., Lopez, R., and Miano, T. M.: Characterization of water extractable organic matter in a deep soil profile, *Chemosphere*, 62, 1583–1590, 10.1016/j.chemosphere.2005.07.065, 2006.
- Cory, R. M., Crump, B. C., Dobkowski, J. A., and Kling, G. W.: Surface exposure to sunlight stimulates CO<sub>2</sub> release from permafrost soil carbon in the Arctic, *Proceedings of the National Academy of Sciences*, 110, 3429–3434, 10.1073/pnas.1214104110, 2013.
- Drake, T. W., Wickland, K. P., Spencer, R. G. M., McKnight, D. M., and Striegl, R. G.: Ancient low-molecular-weight organic acids in permafrost fuel rapid carbon dioxide production upon thaw, *PROCEEDINGS OF THE NATIONAL ACADEMY OF SCIENCES OF THE UNITED STATES OF AMERICA*, 112, 13946–13951, 10.1073/pnas.1511705112, 2015.
- Dutta, K., Schuur, E. A. G., Neff, J. C., and Zimov, S. A.: Potential carbon release from permafrost soils of Northeastern Siberia, *Global Change Biology*, 12, 2336–2351, 10.1111/j.1365-2486.2006.01259.x, 2006.
- Fellman, J. B., D’Amore, D. V., Hood, E., and Boone, R. D.: Fluorescence characteristics and biodegradability of dissolved organic matter in forest and wetland soils from coastal temperate watersheds in southeast Alaska, *Biogeochemistry*, 88, 169–184, 10.1007/s10533-008-9203-x, 2008.
- Fouche, J., Christiansen, C. T., Lafreniere, M. J., Grogan, P., and Lamoureux, S. F.: Canadian permafrost stores large pools of ammonium and optically distinct dissolved organic matter, *Nat Commun*, 11, 4500, 10.1038/s41467-020-18331-w, 2020.
- Frías, J., Ribas, F., and Lucena, F.: Comparison of methods for the measurement of biodegradable organic carbon and assimilable organic carbon in water, *Water Research*, 29, 2785–2788, [https://doi.org/10.1016/0043-1354\(95\)00074-U](https://doi.org/10.1016/0043-1354(95)00074-U), 1995.
- Gao, Z., Niu, F., Wang, Y., Lin, Z., and Wang, W.: Suprapermafrost groundwater flow and exchange around a thermokarst lake on the Qinghai–Tibet Plateau, China, *Journal of Hydrology*, 593, 10.1016/j.jhydrol.2020.125882, 2021.
- Guggenberger, G. and Zech, W.: Dissolved organic carbon in forest floor leachates: simple degradation products or humic substances?, *Science of The Total Environment*, 152, 37–47, 10.1016/0048-9697(94)90549-5, 1994.
- He, C., Chen, W.-M., Chen, C.-M., and Shi, Q.: Molecular transformation of dissolved organic matter in refinery wastewaters: Characterized by FT-ICR MS coupled with electrospray ionization and atmospheric pressure photoionization, *Petroleum Science*, 20, 590–599, 10.1016/j.petsci.2022.09.035, 2023.
- Heffernan, L., Kothawala, D. N., and Tranvik, L. J.: Terrestrial dissolved organic carbon in northern permafrost, *The Cryosphere*, 18, 1443–1465, 2024.
- Helms, J. R., Stubbins, A., Ritchie, J. D., Minor, E. C., Kieber, D. J., and Mopper, K.: Absorption spectral slopes and slope ratios as indicators of molecular weight, source, and photobleaching of chromophoric dissolved organic matter, *Limnology and Oceanography*, 53, 955–969, 10.4319/lo.2008.53.3.0955, 2008.
- Hope, D., Billett, M. F., and Cresser, M. S.: A review of the export of carbon in river water: fluxes and processes, *Environ Pollut*, 84, 301–324, 10.1016/0269-7491(94)90142-2, 1994.
- Hu, G., Fang, H., Liu, G., Zhao, L., Wu, T., Li, R., and Wu, X.: Soil carbon and nitrogen in the active





- layers of the permafrost regions in the Three Rivers' Headstream, *Environmental Earth Sciences*, 72, 5113-5122, 10.1007/s12665-014-3382-7, 2014.
- Huang, W., Deng, X., Lin, Y., and Jiang, Q. o.: An Econometric Analysis of Causes of Forestry Area Changes in Northeast China, *Procedia Environmental Sciences*, 2, 557-565, 10.1016/j.proenv.2010.10.060, 2010.
- Jiang, H., Apps, M. J., Peng, C., Zhang, Y., and Liu, J.: Modelling the influence of harvesting on Chinese boreal forest carbon dynamics, *Forest Ecology and Management*, 169, 65-82, 10.1016/s0378-1127(02)00299-2, 2002.
- Jiang, P., Ma, B., Ni, M., Yuan, D., and Li, S.: Insights into dissolved organic carbon biodegradation process and influencing factors in shallow lakes in a metropolitan, China, *Process Safety and Environmental Protection*, 188, 193-203, 10.1016/j.psep.2024.05.102, 2024.
- Jones, D. and Willett, V.: Experimental evaluation of methods to quantify dissolved organic nitrogen (DON) and dissolved organic carbon (DOC) in soil, *Soil Biology and Biochemistry*, 38, 991-999, 10.1016/j.soilbio.2005.08.012, 2006.
- Kaiser, K. and Kalbitz, K.: Cycling downwards – dissolved organic matter in soils, *Soil Biology and Biochemistry*, 52, 29-32, 10.1016/j.soilbio.2012.04.002, 2012.
- Kalbitz, K., Schmerwitz, J., Schwesig, D., and Matzner, E.: Biodegradation of soil-derived dissolved organic matter as related to its properties, *Geoderma*, 113, 273-291, 10.1016/s0016-7061(02)00365-8, 2003a.
- Kalbitz, K., Schwesig, D., Schmerwitz, J., Kaiser, K., Haumaier, L., Glaser, B., Ellerbrock, R., and Leinweber, P.: Changes in properties of soil-derived dissolved organic matter induced by biodegradation, *Soil Biology and Biochemistry*, 35, 1129-1142, 10.1016/s0038-0717(03)00165-2, 2003b.
- Kaplan, L. A. and Newbold, J. D.: Measurement of streamwater biodegradable dissolved organic carbon with a plug-flow bioreactor, *Water Research*, 29, 2696-2706, [https://doi.org/10.1016/0043-1354\(95\)00135-8](https://doi.org/10.1016/0043-1354(95)00135-8), 1995.
- Kasischke, E. S., Christensen, N. L., and Stocks, B. J.: Fire, Global Warming, and the Carbon Balance of Boreal Forests, *Ecological Applications*, 5, 437-451, 10.2307/1942034, 1995.
- Kirk, P. L.: Kjeldahl Method for Total Nitrogen, *Analytical Chemistry*, 22, 354-358, 10.1021/ac60038a038, 1950.
- Kothawala, D. N., Stedmon, C. A., Muller, R. A., Weyhenmeyer, G. A., Kohler, S. J., and Tranvik, L. J.: Controls of dissolved organic matter quality: evidence from a large-scale boreal lake survey, *Glob Chang Biol*, 20, 1101-1114, 10.1111/gcb.12488, 2014.
- Koven, C. D., Lawrence, D. M., and Riley, W. J.: Permafrost carbon-climate feedback is sensitive to deep soil carbon decomposability but not deep soil nitrogen dynamics, *Proc Natl Acad Sci U S A*, 112, 3752-3757, 10.1073/pnas.1415123112, 2015.
- Li, K.-y., Zhao, Y.-y., Yuan, X.-l., Zhao, H.-b., Wang, Z.-h., Li, S.-x., and Malhi, S. S.: Comparison of Factors Affecting Soil Nitrate Nitrogen and Ammonium Nitrogen Extraction, *Communications in Soil Science and Plant Analysis*, 43, 571-588, 10.1080/00103624.2012.639108, 2012.
- Liang, G., Stefanski, A., Eddy, W. C., Bermudez, R., Montgomery, R. A., Hobbie, S. E., Rich, R. L., and Reich, P. B.: Soil respiration response to decade-long warming modulated by soil moisture in a boreal forest, *Nature Geoscience*, 17, 905-911, 10.1038/s41561-024-01512-3, 2024.
- Lv, J., Han, R., Luo, L., Zhang, X., and Zhang, S.: A Novel Strategy to Evaluate the Aromaticity Degree of Natural Organic Matter Based on Oxidization-Induced Chemiluminescence, *Environmental Science & Technology*, 54, 4171-4179, 10.1021/acs.est.9b07499, 2020.



- 510 Ma, Q., Jin, H., Yu, C., and Bense, V. F.: Dissolved organic carbon in permafrost regions: A review,  
 511 Science China Earth Sciences, 62, 349-364, 10.1007/s11430-018-9309-6, 2019.
- 512 Mann, P. J., Spencer, R. G. M., Hernes, P. J., Six, J., Aiken, G. R., Tank, S. E., McClelland, J. W., Butler,  
 513 K. D., Dyda, R. Y., and Holmes, R. M.: Pan-Arctic Trends in Terrestrial Dissolved Organic Matter from  
 514 Optical Measurements, Frontiers in Earth Science, 4, 10.3389/feart.2016.00025, 2016.
- 515 Margesin, R.: Permafrost soils, Springer Science & Business Media 2008.
- 516 Mentges, M. I., Reichert, J. M., Rodrigues, M. F., Awe, G. O., and Mentges, L. R.: Capacity and intensity  
 517 soil aeration properties affected by granulometry, moisture, and structure in no-tillage soils, Geoderma,  
 518 263, 47-59, 10.1016/j.geoderma.2015.08.042, 2016.
- 519 Michalzik, B., Tipping, E., Mulder, J., Lancho, J. F. G., Matzner, E., Bryant, C. L., Clarke, N., Loftis, S.,  
 520 and Esteban, M. A. V.: Modelling the production and transport of dissolved organic carbon in forest soils,  
 521 Biogeochemistry, 66, 241-264, 10.1023/b:Biog.00000005329.68861.27, 2003.
- 522 Moore, T. R.: Dissolved organic carbon in a northern boreal landscape, Global Biogeochemical Cycles,  
 523 17, 10.1029/2003gb002050, 2003.
- 524 Mu, C. C., Abbott, B. W., Wu, X. D., Zhao, Q., Wang, H. J., Su, H., Wang, S. F., Gao, T. G., Guo, H.,  
 525 Peng, X. Q., and Zhang, T. J.: Thaw Depth Determines Dissolved Organic Carbon Concentration and  
 526 Biodegradability on the Northern Qinghai-Tibetan Plateau, Geophysical Research Letters, 44, 9389-9399,  
 527 10.1002/2017gl075067, 2017.
- 528 Murphy, K. R., Stedmon, C. A., Waite, T. D., and Ruiz, G. M.: Distinguishing between terrestrial and  
 529 autochthonous organic matter sources in marine environments using fluorescence spectroscopy, Marine  
 530 Chemistry, 108, 40-58, 10.1016/j.marchem.2007.10.003, 2008.
- 531 Neff, J. C. and Asner, G. P.: Dissolved Organic Carbon in Terrestrial Ecosystems: Synthesis and a Model,  
 532 Ecosystems, 4, 29-48, 10.1007/s100210000058, 2001.
- 533 Nelson, D. W. and Sommers, L. E.: Total Carbon, Organic Carbon, and Organic Matter, in: Methods of  
 534 Soil Analysis, 961-1010, <https://doi.org/10.2136/sssabookser5.3.c34>, 1996.
- 535 Ohlson, M., Dahlberg, B., Økland, T., Brown, K. J., and Halvorsen, R.: The charcoal carbon pool in  
 536 boreal forest soils, Nature Geoscience, 2, 692-695, 10.1038/ngeo617, 2009.
- 537 Olefeldt, D. and Roulet, N. T.: Effects of permafrost and hydrology on the composition and transport of  
 538 dissolved organic carbon in a subarctic peatland complex, Journal of Geophysical Research:  
 539 Biogeosciences, 117, 10.1029/2011jg001819, 2012.
- 540 Olefeldt, D., Persson, A., and Turetsky, M. R.: Influence of the permafrost boundary on dissolved organic  
 541 matter characteristics in rivers within the Boreal and Taiga plains of western Canada, Environmental  
 542 Research Letters, 9, 10.1088/1748-9326/9/3/035005, 2014.
- 543 Öquist, M. G., Bishop, K., Grelle, A., Klemetsson, L., Köhler, S. J., Laudon, H., Lindroth, A., Ottosson  
 544 Löfvenius, M., Wallin, M. B., and Nilsson, M. B.: The Full Annual Carbon Balance of Boreal Forests Is  
 545 Highly Sensitive to Precipitation, Environmental Science & Technology Letters, 1, 315-319,  
 546 10.1021/ez500169j, 2014.
- 547 Panneer Selvam, B., Laudon, H., Guillemette, F., and Berggren, M.: Influence of soil frost on the  
 548 character and degradability of dissolved organic carbon in boreal forest soils, Journal of Geophysical  
 549 Research: Biogeosciences, 121, 829-840, 10.1002/2015jg003228, 2016.
- 550 Panneer Selvam, B., Lapierre, J. F., Guillemette, F., Voigt, C., Lamprecht, R. E., Biasi, C., Christensen,  
 551 T. R., Martikainen, P. J., and Berggren, M.: Degradation potentials of dissolved organic carbon (DOC)  
 552 from thawed permafrost peat, Sci Rep, 7, 45811, 10.1038/srep45811, 2017.
- 553 Peng, R., Liu, H., Anenkhonov, O. A., Sandanov, D. V., Korolyuk, A. Y., Shi, L., Xu, C., Dai, J., and



- 554 Wang, L.: Tree growth is connected with distribution and warming-induced degradation of permafrost in  
 555 southern Siberia, *Glob Chang Biol*, 28, 5243-5253, 10.1111/gcb.16284, 2022.
- 556 Pengerud, A., Dignac, M.-F., Certini, G., Strand, L. T., Forte, C., and Rasse, D. P.: Soil organic matter  
 557 molecular composition and state of decomposition in three locations of the European Arctic,  
 558 *Biogeochemistry*, 135, 277-292, 10.1007/s10533-017-0373-2, 2017.
- 559 Ping, C. L., Jastrow, J. D., Jorgenson, M. T., Michaelson, G. J., and Shur, Y. L.: Permafrost soils and  
 560 carbon cycling, *Soil*, 1, 147-171, 10.5194/soil-1-147-2015, 2015.
- 561 Qu, W., Li, J., Han, G., Wu, H., Song, W., and Zhang, X.: Effect of salinity on the decomposition of soil  
 562 organic carbon in a tidal wetland, *Journal of Soils and Sediments*, 19, 609-617, 10.1007/s11368-018-  
 563 2096-y, 2018.
- 564 Ran, Y., Li, X., Cheng, G., Zhang, T., Wu, Q., Jin, H., and Jin, R.: Distribution of Permafrost in China:  
 565 An Overview of Existing Permafrost Maps, *Permafrost and Periglacial Processes*, 23, 322-333,  
 566 10.1002/ppp.1756, 2012.
- 567 Randerson, J. T., Liu, H., Flanner, M. G., Chambers, S. D., Jin, Y., Hess, P. G., Pfister, G., Mack, M. C.,  
 568 Treseder, K. K., Welp, L. R., Chapin, F. S., Harden, J. W., Goulden, M. L., Lyons, E., Neff, J. C., Schuur,  
 569 E. A., and Zender, C. S.: The impact of boreal forest fire on climate warming, *Science*, 314, 1130-1132,  
 570 10.1126/science.1132075, 2006.
- 571 Raudina, T. V., Loiko, S. V., Lim, A. G., Krickov, I. V., Shirokova, L. S., Istigechev, G. I., Kuzmina, D.  
 572 M., Kulizhsky, S. P., Vorobyev, S. N., and Pokrovsky, O. S.: Dissolved organic carbon and major and  
 573 trace elements in peat porewater of sporadic, discontinuous, and continuous permafrost zones of western  
 574 Siberia, *Biogeosciences*, 14, 3561-3584, 10.5194/bg-14-3561-2017, 2017.
- 575 Roehm, C. L., Giesler, R., and Karlsson, J.: Bioavailability of terrestrial organic carbon to lake bacteria:  
 576 The case of a degrading subarctic permafrost mire complex, *Journal of Geophysical Research*, 114,  
 577 10.1029/2008jg000863, 2009.
- 578 Schirrmeister, L., Kunitsky, V., Grosse, G., Wetterich, S., Meyer, H., Schwamborn, G., Babiy, O.,  
 579 Derevyagin, A., and Siegert, C.: Sedimentary characteristics and origin of the Late Pleistocene Ice  
 580 Complex on north-east Siberian Arctic coastal lowlands and islands – A review, *Quaternary International*,  
 581 241, 3-25, 10.1016/j.quaint.2010.04.004, 2011.
- 582 Sgroi, M., Anumol, T., Roccaro, P., Vagliasindi, F. G. A., and Snyder, S. A.: Modeling emerging  
 583 contaminants breakthrough in packed bed adsorption columns by UV absorbance and fluorescing  
 584 components of dissolved organic matter, *Water Res*, 145, 667-677, 10.1016/j.watres.2018.09.018, 2018.
- 585 Song, X., Wang, G., Ran, F., Huang, K., Sun, J., and Song, C.: Soil moisture as a key factor in carbon  
 586 release from thawing permafrost in a boreal forest, *Geoderma*, 357, 10.1016/j.geoderma.2019.113975,  
 587 2020.
- 588 Sparks, D. L., Page, A. L., Helmke, P. A., and Loeppert, R. H.: *Methods of soil analysis, part 3: Chemical*  
 589 *methods*, John Wiley & Sons 2020.
- 590 Spencer, R. G. M., Mann, P. J., Dittmar, T., Eglinton, T. I., McIntyre, C., Holmes, R. M., Zimov, N., and  
 591 Stubbins, A.: Detecting the signature of permafrost thaw in Arctic rivers, *Geophysical Research Letters*,  
 592 42, 2830-2835, 10.1002/2015gl063498, 2015.
- 593 Strauss, J., Schirrmeister, L., Grosse, G., Fortier, D., Hugelius, G., Knoblauch, C., Romanovsky, V.,  
 594 Schädel, C., Schneider von Deimling, T., Schuur, E. A. G., Shmelev, D., Ulrich, M., and Veremeeva, A.:  
 595 Deep Yedoma permafrost: A synthesis of depositional characteristics and carbon vulnerability, *Earth-*  
 596 *Science Reviews*, 172, 75-86, 10.1016/j.earscirev.2017.07.007, 2017.
- 597 Sun, B., Li, Y., Song, M., Li, R., Li, Z., Zhuang, G., Bai, Z., and Zhuang, X.: Molecular characterization



598 of the composition and transformation of dissolved organic matter during the semi-permeable membrane  
 599 covered hyperthermophilic composting, *Journal of Hazardous Materials*, 425,  
 600 10.1016/j.jhazmat.2021.127496, 2022.

601 Takaki, Y., Hattori, K., and Yamashita, Y.: Factors Controlling the Spatial Distribution of Dissolved  
 602 Organic Matter With Changes in the C/N Ratio From the Upper to Lower Reaches of the Ishikari River,  
 603 Japan, *Frontiers in Earth Science*, 10, 10.3389/feart.2022.826907, 2022.

604 Thurman, E. M.: Organic geochemistry of natural waters, Springer Science & Business Media,  
 605 <https://doi-org.proxy.library.carleton.ca/10.1007/978-94-009-5095-5>, 2012.

606 Vonk, J. E., Tank, S. E., Mann, P. J., Spencer, R. G. M., Treat, C. C., Striegl, R. G., Abbott, B. W., and  
 607 Wickland, K. P.: Biodegradability of dissolved organic carbon in permafrost soils and aquatic systems: a  
 608 meta-analysis, *Biogeosciences*, 12, 6915-6930, 10.5194/bg-12-6915-2015, 2015.

609 Vos, C., Don, A., Prietz, R., Heidkamp, A., and Freibauer, A.: Field-based soil-texture estimates could  
 610 replace laboratory analysis, *Geoderma*, 267, 215-219, 10.1016/j.geoderma.2015.12.022, 2016.

611 Walker, S. A., Amon, R. M. W., and Stedmon, C. A.: Variations in high-latitude riverine fluorescent  
 612 dissolved organic matter: A comparison of large Arctic rivers, *Journal of Geophysical Research:*  
 613 *Biogeosciences*, 118, 1689-1702, 10.1002/2013jg002320, 2013.

614 Walz, J., Knoblauch, C., Böhme, L., and Pfeiffer, E.-M.: Regulation of soil organic matter decomposition  
 615 in permafrost-affected Siberian tundra soils - Impact of oxygen availability, freezing and thawing,  
 616 temperature, and labile organic matter, *Soil Biology and Biochemistry*, 110, 34-43,  
 617 10.1016/j.soilbio.2017.03.001, 2017.

618 Wang, Y., Wang, Y., Han, L., McKenna, A. M., Kellerman, A. M., Spencer, R. G. M., Yang, Y., and Xu,  
 619 Y.: Concentration and compositional controls on degradation of permafrost-derived dissolved organic  
 620 matter on the Qinghai-Tibetan Plateau, *Limnology and Oceanography Letters*, 10.1002/lol2.10388, 2024.

621 Ward, C. P. and Cory, R. M.: Chemical composition of dissolved organic matter draining permafrost soils,  
 622 *Geochimica et Cosmochimica Acta*, 167, 63-79, 10.1016/j.gca.2015.07.001, 2015.

623 Weishaar, J. L., Aiken, G. R., Bergamaschi, B. A., Fram, M. S., Fujii, R., and Mopper, K.: Evaluation of  
 624 specific ultraviolet absorbance as an indicator of the chemical composition and reactivity of dissolved  
 625 organic carbon, *Environ Sci Technol*, 37, 4702-4708, 10.1021/es030360x, 2003.

626 Wickland, K. P., Neff, J. C., and Aiken, G. R.: Dissolved Organic Carbon in Alaskan Boreal Forest:  
 627 Sources, Chemical Characteristics, and Biodegradability, *Ecosystems*, 10, 1323-1340, 10.1007/s10021-  
 628 007-9101-4, 2007.

629 Wild, B., Schneckner, J., Alves, R. J., Barsukov, P., Barta, J., Capek, P., Gentsch, N., Gittel, A.,  
 630 Guggenberger, G., Lashchinskiy, N., Mikutta, R., Rusalimova, O., Santruckova, H., Shibistova, O., Urich,  
 631 T., Watzka, M., Zrazhevskaya, G., and Richter, A.: Input of easily available organic C and N stimulates  
 632 microbial decomposition of soil organic matter in arctic permafrost soil, *Soil Biol Biochem*, 75, 143-151,  
 633 10.1016/j.soilbio.2014.04.014, 2014.

634 Wu, M. H., Chen, S. Y., Chen, J. W., Xue, K., Chen, S. L., Wang, X. M., Chen, T., Kang, S. C., Rui, J. P.,  
 635 Thies, J. E., Bardgett, R. D., and Wang, Y. F.: Reduced microbial stability in the active layer is associated  
 636 with carbon loss under alpine permafrost degradation, *Proc Natl Acad Sci U S A*, 118,  
 637 10.1073/pnas.2025321118, 2021.

638 Yang, J., Zhan, C., Li, Y., Zhou, D., Yu, Y., and Yu, J.: Effect of salinity on soil respiration in relation to  
 639 dissolved organic carbon and microbial characteristics of a wetland in the Liaohe River estuary, Northeast  
 640 China, *Science of The Total Environment*, 642, 946-953, 10.1016/j.scitotenv.2018.06.121, 2018.

641 Ye, L., Wu, X., Liu, B., Yan, D., and Kong, F.: Dynamics and sources of dissolved organic carbon during



642 phytoplankton bloom in hypereutrophic Lake Taihu (China), *Limnologia*, 54, 5-13,  
 643 10.1016/j.limno.2015.05.003, 2015.  
 644 Zhang, R. V., Zabolotnik, S. I., and Zabolotnik, P. S.: Assessment of the thermal effect of large industrial  
 645 buildings on permafrost foundation soils in Yakutsk, *Research in Cold and Arid Regions*, 15, 262-267,  
 646 <https://doi.org/10.1016/j.rcar.2023.12.001>, 2023.  
 647 Zhong, S., Li, B., Hou, B., Xu, X., Hu, J., Jia, R., Yang, S., Zhou, S., and Ni, J.: Structure, stability, and  
 648 potential function of groundwater microbial community responses to permafrost degradation on varying  
 649 permafrost of the Qinghai-Tibet Plateau, *Sci Total Environ*, 875, 162693,  
 650 10.1016/j.scitotenv.2023.162693, 2023.  
 651 Zhou, X., Ma, A., Chen, X., Zhang, Q., Guo, X., and Zhuang, G.: Climate Warming-Driven Changes in  
 652 the Molecular Composition of Soil Dissolved Organic Matter Across Depth: A Case Study on the Tibetan  
 653 Plateau, *Environmental Science & Technology*, 10.1021/acs.est.3c04899, 2023.  
 654 Zou, T. and Yoshino, K.: Environmental vulnerability evaluation using a spatial principal components  
 655 approach in the Daxing'anling region, China, *Ecological Indicators*, 78, 405-415,  
 656 10.1016/j.ecolind.2017.03.039, 2017.

657